

Controlling photonic spin Hall effect based on tunable surface plasmon resonance with an N -type coherent medium

Ren-Gang Wan^{1,2,*} and M. Suhail Zubairy^{2,†}¹*School of Physics and Information Technology, Shaanxi Normal University, Xi'an 710062, China*²*Institute for Quantum Science and Engineering (IQSE) and Department of Physics and Astronomy, Texas A&M University, College Station, Texas 77843-4242, USA*

(Received 12 November 2019; accepted 9 March 2020; published 26 March 2020)

We propose a scheme to control the spin Hall effect (SHE) of light reflected from a Kretschmann configuration containing an N -type coherent atomic medium. Owing to the excitation of surface plasmon resonance (SPR), enhanced spin splitting occurs in the reflection dip for TM-polarized incident light. The magnitude and sign of the transverse shifts of spin components depend on the system internal damping which is closely related to the absorption coefficient of atoms. There is an optimal absorption around which the spin components undergo large transverse displacements. We also show that the direction of the photonic spin accumulations can be switched between positive and negative values by adjusting the system parameters. In addition, the resonance angle of SPR varies linearly with the refractivity of the medium. We can therefore coherently control the peak position of the transverse shift. Compared to the conventional SPR-based systems, the proposed scheme provides a more flexible pathway for manipulating and enhancing the SHE of light without changing the structure. This tunable SHE may find applications in spin photonic devices.

DOI: [10.1103/PhysRevA.101.033837](https://doi.org/10.1103/PhysRevA.101.033837)

I. INTRODUCTION

The atomic coherence and the quantum interference effects induced by the interaction between light and matter lie at the heart of many applications of quantum optics. The relevant research has attracted significant interest due to their promising applications in quantum information and optical communication. Based on the quantum interference effect in multilevel atomic system, the linear and nonlinear optical response can be effectively manipulated, thereby leading to many important phenomena, such as amplification without inversion [1–3], electromagnetically induced transparency [4–6], slow and fast light [7,8], quantum memory [9,10], optical solitons [11,12], giant Kerr nonlinearity [13–15], and enhanced multiwave mixing [16–18]. Recently, the atomic coherence effect is exploited to manipulate the Goos-Hänchen (GH) effect of a light beam reflected or refracted from the interface of different media and structures [19–24].

The GH shift refers to the lateral displacement of a light beam from its predicted geometric optics path [25]. There is also a spin-dependent transverse shift of the wave packet perpendicular to the incident plane. It is known as the photonic spin Hall effect (SHE) [26–28] and is sometimes referred to as the Imbert-Fedorov effect [29,30]. The SHE of light can be regarded as an optical analog of the SHE of electrons by replacing the electron spin and the electric potential with the photon spin and the refractive index gradient. Due to the potential applications in spin manipulation in quantum

information and precision metrology, the SHE of light has attracted the interest of researchers. In general, the splitting of two spin components is too small to be directly measured. By using the weak measurement technique, the transverse shift of refracted light was first observed [31]. It has been demonstrated experimentally that the SHE of light can be enhanced near the Brewster angle on reflection [32,33]. Recently, a variety of physical systems have been proposed to enhance and control the spatial separation of spin components, such as multilayer nanostructures [34–38], metal film [39], epsilon- and mu-near-zero slab [40,41], metamaterials [42,43], graphene [44–46], and surface plasmon resonance (SPR) systems [47–50]. The transverse shift of light beams has also been studied in the interface or structure with coherent media [51,52]. However, the displacements were not large enough in such systems.

The Kretschmann configuration has been widely utilized to achieve a giant transverse shift owing to the excitation of SPR [47–50]. In the sharp resonance dip, the TM-polarized light beam splits into two spin components in the direction perpendicular to the incident plane. The magnitude and sign of spin-dependent shift can be tuned by the thickness of the metal layer. However, this is difficult to do and we do not have the needed flexibility.

In this paper, we propose a hybrid system of SPR structure and coherent medium to control the photonic SHE. When the wave vector of incident light matches that of the surface plasmon, the light energy penetrates into the structure resulting in attenuated total reflection. By modulating the absorption of the medium, a large ratio between the reflection coefficients of TE and TM polarizations can be obtained. As a result, the spin components of a TM-polarized light beam

*wrg@snnu.edu.cn

†zubairy@physics.tamu.edu

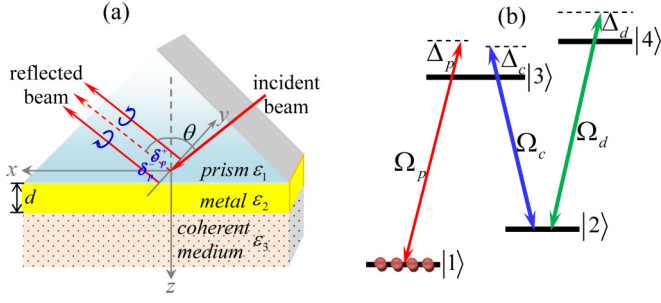


FIG. 1. (a) Schematic setup of a three-layer Kretschmann configuration composed of a prism, a metal film, and a coherent atomic medium. Spin-dependent splitting occurs for a TM-polarized incident light reflected from the prism-metal interface. (b) Four-level N -type atomic system driven by three lasers: probe field, coupling field, and driving field.

are largely separated in the transverse direction. Therefore the magnitude and sign of the transverse shift can be manipulated conveniently based on the atomic coherence effect. Moreover, the SPR angle as well as the peak position of the transverse shift is closely related to the refractive part of the susceptibility of the atomic medium, which can also be tuned coherently. Compared with other SPR-based schemes, the coherent medium provides more flexibility for manipulating the SHE of light. These findings are useful for designing new spin-based optical devices.

II. MODEL AND EQUATIONS

We consider a three-layer structure in the Kretschmann configuration as shown in Fig. 1(a). It consists of a prism, a thin metal film with thickness d , and a coherent medium consisting of a four-level atomic system as shown in Fig. 1(b). Their permittivities (dielectric constants) are ϵ_1 , ϵ_2 , and ϵ_3 , respectively. The dielectric constant ϵ_3 is derived later in this section. When a TM-polarized light beam is incident on the prism-metal interface, SPR can be excited at a certain angle. The attenuation of reflection in the resonance dip gives rise to an enhancement of photonic SHE. The left- and right-circular polarization components of the reflected light beam are spatially split in the direction perpendicular to the plane of incidence. The corresponding transverse displacements δ_p^+ and δ_p^- can be derived from the reflective coefficients of the three-layer structure [34,49,50]:

$$\delta_p^\pm = \mp \frac{k_1 w_0^2 [1 + \frac{|r_s|}{|r_p|} \cos(\varphi_s - \varphi_p)] \cot \theta}{k_1^2 w_0^2 + \left| \frac{\partial \ln r_p}{\partial \theta} \right|^2 + \left| \left(1 + \frac{r_s}{r_p}\right) \cot \theta \right|^2}. \quad (1)$$

Here $k_1 = \sqrt{\epsilon_1} k_0$ and $k_0 = 2\pi/\lambda$ denotes the wave vector with λ being the light wavelength. w_0 represents the radius of the waist of the incident beam, r_p and r_s refer to the complex reflection coefficients for TM and TE light beams, and φ_p and φ_s correspond to the phase differences between the incident and reflected light fields. For the SPR structure discussed here, the reflection coefficients r_p and r_s can be written as

$$r_{p,s} = \frac{r_{p,s}^{12} + r_{p,s}^{23} e^{2ik_z d}}{1 + r_{p,s}^{12} r_{p,s}^{23} e^{2ik_z d}}, \quad (2)$$

where $r_{p,s}^{ij}$ is the Fresnel's reflection coefficient at the i - j interface given by

$$r_p^{ij} = \frac{k_{iz}/\epsilon_i - k_{jz}/\epsilon_j}{k_{iz}/\epsilon_i + k_{jz}/\epsilon_j}, \quad (3)$$

$$r_s^{ij} = \frac{k_{iz} - k_{jz}}{k_{iz} + k_{jz}}. \quad (4)$$

Here $k_{iz} = \sqrt{k_0^2 \epsilon_i - k_x^2}$ represents the normal wave vector in the corresponding layer, and $k_x = \sqrt{\epsilon_1} k_0 \sin \theta$ is the wave vector along the x direction.

For the Kretschmann configuration, TE-polarized light is almost totally reflected; i.e., $|r_s| \approx 1$. Nevertheless, SPR can be excited by TM-polarized light and results in attenuated total reflection. The resonance angle and the reflectivity of the resonance dip are sensitive to the complex permittivity of medium. Next we derive an expression for the susceptibility of the coherent medium, and hence the dielectric constant ϵ_3 . Considering a four-level N -type atomic system as depicted in Fig. 1(b), a weak probe field E_p with Rabi frequency Ω_p and detuning $\Delta_p = \omega_p - \omega_{31}$ couples the transition $|1\rangle \leftrightarrow |3\rangle$, the transition $|2\rangle \leftrightarrow |3\rangle$ is driven by a coupling field E_c with Rabi frequency Ω_c and detuning $\Delta_c = \omega_c - \omega_{32}$, and a driving field E_d with Rabi frequency Ω_d and detuning $\Delta_d = \omega_d - \omega_{42}$ interacts with the transition $|2\rangle \leftrightarrow |4\rangle$. The Rabi frequencies are defined as $\Omega_p = \mu_{13} E_p / (2\hbar)$, $\Omega_c = \mu_{23} E_c / (2\hbar)$, and $\Omega_d = \mu_{24} E_d / (2\hbar)$, where μ_{ij} is the electric-dipole moment of the corresponding transition.

Under the electric-dipole and rotating-wave approximations, the Hamiltonian of the system in the interaction picture can be expressed as

$$H_{\text{int}} = -\hbar[(\Delta_p - \Delta_c)|2\rangle\langle 2| + \Delta_p|3\rangle\langle 3| + (\Delta_p - \Delta_c + \Delta_d)|4\rangle\langle 4| + (\Omega_p|3\rangle\langle 1| + \Omega_c|3\rangle\langle 2| + \Omega_d|4\rangle\langle 2| + \text{H.c.})]. \quad (5)$$

The atomic dynamics is governed by the Liouville equation $\dot{\rho} = -(i/\hbar)[H_{\text{int}}, \rho] + L_p$ where L_p represents the relaxation process. Then the equations of motion of the density matrix elements can be written as

$$\dot{\rho}_{11} = i\Omega_p \rho_{31} - i\Omega_p \rho_{13} + \Gamma_{31} \rho_{33} + \Gamma_{41} \rho_{44}, \quad (6)$$

$$\dot{\rho}_{22} = i\Omega_c \rho_{32} - i\Omega_c \rho_{23} + i\Omega_d \rho_{42} - i\Omega_d \rho_{24} + \Gamma_{32} \rho_{33} + \Gamma_{42} \rho_{44}, \quad (7)$$

$$\dot{\rho}_{33} = i\Omega_p \rho_{13} - i\Omega_p \rho_{31} + i\Omega_c \rho_{23} - i\Omega_c \rho_{32} - (\Gamma_{31} + \Gamma_{32}) \rho_{33}, \quad (8)$$

$$\dot{\rho}_{21} = i\Omega_c \rho_{31} - i\Omega_p \rho_{23} + i\Omega_d \rho_{41} + i[(\Delta_p - \Delta_c) + i\gamma_{21}] \rho_{21}, \quad (9)$$

$$\dot{\rho}_{31} = i\Omega_p \rho_{11} - i\Omega_p \rho_{33} + i\Omega_c \rho_{21} + i\Omega_d \rho_{41} + i[\Delta_p + i(\Gamma_{31} + \Gamma_{32})/2] \rho_{31}, \quad (10)$$

$$\dot{\rho}_{41} = i\Omega_d \rho_{21} - i\Omega_p \rho_{43} + i[(\Delta_p - \Delta_c + \Delta_d) + i(\Gamma_{41} + \Gamma_{42})/2] \rho_{41}, \quad (11)$$

$$\begin{aligned} \dot{\rho}_{32} = & i\Omega_c \rho_{22} - i\Omega_c \rho_{33} + i\Omega_p \rho_{12} - i\Omega_d \rho_{34} \\ & + i[\Delta_c + i(\Gamma_{31} + \Gamma_{32})/2]\rho_{32}, \end{aligned} \quad (12)$$

$$\begin{aligned} \dot{\rho}_{42} = & i\Omega_d \rho_{22} - i\Omega_d \rho_{44} - i\Omega_c \rho_{43} \\ & + i[\Delta_d + i(\Gamma_{41} + \Gamma_{42})/2]\rho_{42}, \end{aligned} \quad (13)$$

$$\begin{aligned} \dot{\rho}_{43} = & i\Omega_d \rho_{23} - i\Omega_p \rho_{41} - i\Omega_c \rho_{42} + i[(\Delta_c - \Delta_d) \\ & + i(\Gamma_{31} + \Gamma_{32} + \Gamma_{41} + \Gamma_{42})/2]\rho_{43}, \end{aligned} \quad (14)$$

where Γ_{31} , Γ_{32} , Γ_{41} , and Γ_{42} represent the decay rates of the corresponding transitions and γ_{21} denotes the decoherence between the two ground states. The above equations are constrained by $\rho_{11} + \rho_{22} + \rho_{33} + \rho_{44} = 1$ and $\rho_{ij} = \rho_{ji}^*$ ($i \neq j$).

The permittivity of the medium, ϵ_3 , can be derived from the susceptibility χ via the relation $\epsilon_3 = 1 + \chi$. We solve the above equations in the steady state in the case of weak probe field. The polarization of the medium is given by $P = \epsilon_0 \chi E_p = N \mu_{31} \rho_{31}$. Then the resulting susceptibility is

$$\chi = -\mathcal{N} \frac{d_{21}d_{41} - \Omega_d^2}{d_{31}(d_{21}d_{41} - \Omega_d^2) - d_{41}\Omega_c^2}, \quad (15)$$

where $d_{21} = (\Delta_p - \Delta_c) + i\gamma_{21}$, $d_{31} = \Delta_p + i\Gamma_3/2$, $d_{41} = (\Delta_p - \Delta_c + \Delta_d) + i\Gamma_4/2$, $\mathcal{N} = N\mu_{13}^2/(2\hbar\epsilon_0)$; N and ϵ_0 refer to the atomic density and dielectric constant in vacuum, respectively; and $\Gamma_3 = \Gamma_{31} + \Gamma_{32}$ and $\Gamma_4 = \Gamma_{41} + \Gamma_{42}$ represent the total decay rates from levels |3) and |4). It is clear that the susceptibility of the medium depends on the parameters of the light field and can be manipulated effectively. This leads to tunable SPR and controllable SHE of light.

III. RESULTS AND DISCUSSIONS

It can be seen from Eq. (1) that the transverse shift depends on the ratio of reflection coefficients $|r_s|/|r_p|$, and the phase difference $\varphi_s - \varphi_p$. For the Kretschmann configuration, SPR can be excited by a TM-polarized light beam incident at the prism-metal interface, resulting in attenuated reflection around the resonance angle, while for the TE-polarized light, it is almost totally reflected; i.e., $|r_s| \approx 1$. In order to obtain a significant SHE of light, efforts should be made to reduce $|r_p|$. According to Kretschmann's theory, the reflectivity of the TM light can be derived from Eq. (2), and is given by

$$|r_p| = |r_{12}| \sqrt{1 - \frac{4\Gamma^{\text{int}}\Gamma^{\text{rad}}}{[k_x - \text{Re}(k_x^0 + \Delta k_x)]^2 + (\Gamma^{\text{int}} + \Gamma^{\text{rad}})^2}}, \quad (16)$$

with

$$k_x^0 = k_0 \sqrt{\frac{\epsilon_2 \epsilon_3}{\epsilon_2 + \epsilon_3}}, \quad (17)$$

$$\Delta k_x = k_0 [r_{12}(k_x = k_x^0)] \left(\frac{2}{\epsilon_3 - \epsilon_2} \right) \left(\frac{\epsilon_2 \epsilon_3}{\epsilon_2 + \epsilon_3} \right)^{3/2} \exp(2ik_{2z}d). \quad (18)$$

Here k_x^0 is the resonance wave vector of the surface plasmon for a semi-infinite metal-medium structure, $k_x^0 + \Delta k_x$ denotes the resonance wave vector of SPR in the prism coupled structure, Δk_x is the perturbation to k_x^0 owing to the prism, $\Gamma^{\text{int}} = \text{Im}(k_x^0)$ represents the internal damping resulting from the absorption loss of the metal and the medium, and $\Gamma^{\text{rad}} = \text{Im}(\Delta k_x)$ represents the radiation damping which has a positive correlation to the thickness of the metal layer. When the resonance condition $k_x = \text{Re}(k_x^0 + \Delta k_x)$ is fulfilled, SPR takes place, leading to a minimum reflectivity which is given by

$$|r_p|_{\text{min}} = |r_{12}| \sqrt{1 - \frac{4\Gamma^{\text{int}}\Gamma^{\text{rad}}}{(\Gamma^{\text{int}} + \Gamma^{\text{rad}})^2}}. \quad (19)$$

The minimum of reflectivity depends on the values of two dampings. It goes to exactly zero when $\Gamma^{\text{int}} = \Gamma^{\text{rad}}$. For the optically thin coherent medium where $|\chi| \ll 1$, Γ^{int} can be written as

$$\Gamma^{\text{int}} \approx \frac{k_0}{2} \sqrt{\frac{1}{\epsilon'_2(\epsilon'_2 + 1)^3}} [\epsilon''_2 + \epsilon'_2 \text{Im}(\chi)], \quad (20)$$

where ϵ'_2 and ϵ''_2 correspond, respectively, to the real and imaginary parts of ϵ_2 . In the derivation of Eq. (20), we have assumed that $|\epsilon'_2| \gg \epsilon''_2$ and $|\epsilon'_2| \gg 1$. It is clear that Γ^{int} is closely related to the imaginary part of the permittivity of the medium. However, Γ^{rad} is not sensitive to the absorption and almost remains constant. Therefore, we can conveniently control the photonic SHE by adjusting the absorption coefficient of the medium. This is in contrast to the other SPR schemes [48–50] where the manipulation of SHE is achieved by tuning the radiation damping via the thickness of the metal film which is not feasible for a fixed configuration.

In the following we present numerical results when cold sodium atoms are considered as the coherent medium. The N -type system can be realized with the D_2 transition hyperfine structure where the wavelength of the probe field is about 589.1 nm. The dielectric constants of the glass prism and the silver film are $\epsilon_1 = 2.25$ and $\epsilon_2 = -13.3 + 0.883i$, respectively. The dielectric constant of the medium is dependent on the parameters of the laser fields, thereby resulting in tunable and enhanced SHE of light upon reflection from the structure. Because the beam shifts for the two circular components are equal in magnitude and opposite in sign, we only presented the transverse shift of one spin component, i.e., δ_p^+ .

First we consider the case where all fields are resonant with the relevant transitions, i.e., $\Delta_p = \Delta_c = \Delta_d = 0$. In Figs. 2(a) and 2(b), we plot the reflectivity and transverse shift as a function of incident angle for different values of the Rabi frequency of the driving field. As can be seen, a reflection dip occurs owing to the excitation of SPR. Around the resonance angle, there is an enhanced transverse shift. Initially, the minimum reflectivity decreases with Ω_d and then is increased gradually. The magnitude of the spin splitting has similar behavior. However, the sign is switched from negative to positive. These results are related to the change in dielectric constant ϵ_3 . Driven by the coupling and driving fields, the upper level |3) splits into three dressed states, $|\pm\rangle = (E_{\pm}|2\rangle + \Omega_c|3\rangle + \Omega_d|4\rangle)/(E_{\pm}^2 + \Omega_c^2 + \Omega_d^2)^{1/2}$

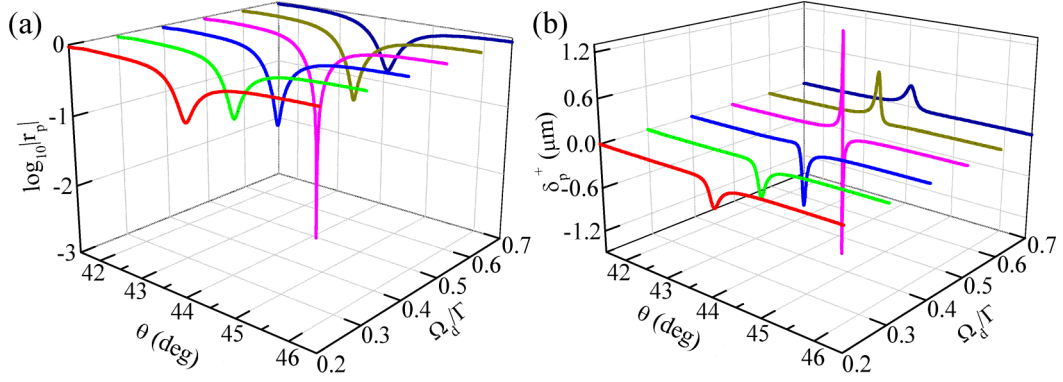


FIG. 2. (a) Reflectivity $|r_p|$ and (b) transverse shift of left-handed circularly polarized light δ_p^+ as a function of incident angle θ with various Rabi frequencies of driving field Ω_d . Parameters are $\varepsilon_1 = 2.25$, $\varepsilon_2 = -13.3 + 0.883i$, $d = 40\text{nm}$, $\Gamma_3 = \Gamma_4 \equiv \Gamma$, $\mathcal{N} = 0.04\Gamma$, $\Delta_p = 0$, $\Delta_c = 0$, $\Delta_d = 0$, and $\Omega_c = 2\Gamma$.

and $|0\rangle = (\Omega_d|3\rangle - \Omega_c|4\rangle)/(\Omega_c^2 + \Omega_d^2)^{1/2}$ with eigenenergies $E_{\pm} = (\Omega_c^2 + \Omega_d^2)^{1/2}$ and $E_0 = 0$, respectively. In the dressed-state picture, the probe field resonantly couples the $|1\rangle \leftrightarrow |0\rangle$ transition, thereby leading to controllable absorption. It follows from Eq. (15) that, on neglecting the decoherence between the ground states, the probe susceptibility is given by

$$\chi = i\mathcal{N} \frac{2\Omega_d^2}{\Omega_c^2\Gamma_4 + \Omega_d^2\Gamma_3}, \quad (21)$$

which is pure imaginary and increases with Ω_d [see Fig. 3(a)]. Then the internal damping Γ^{int} changes accordingly [see Fig. 3(b)]. It becomes equal to Γ^{rad} as the absorption reaches an optimal value [$\text{Im}(\varepsilon_3) \approx 0.0047$], and we can simultaneously obtain large positive and negative transverse shifts with nearly the same magnitudes as shown in Fig. 3(c). In this case, the phase has a sudden change at the resonance angle for TM light and the reflectivity goes to zero, resulting in a severely distorted reflected beam. Around the optimal absorption, the reflection ratio $|r_s|/|r_p|$ is greatly enhanced and results in enhanced spin splitting. The direction of the spin accumulations is related to the phase difference $\varphi_s - \varphi_p$ and depends on the internal damping. On the condition of $\Gamma^{\text{int}} < \Gamma^{\text{rad}}$, the left-hand circular component of the reflected beam is transversely displaced to the negative direction of

the y axis. However, a positive transverse shift occurs when $\Gamma^{\text{int}} > \Gamma^{\text{rad}}$ [see Fig. 3(c)].

The absorption can also be controlled via the coupling field. As the Rabi frequency Ω_c is increased, the probe field remains resonant with the dressed state $|0\rangle$. However, the corresponding electric-dipole moment [$\mu_{01} = \Omega_d\mu_{31}/(\Omega_c^2 + \Omega_d^2)^{1/2}$] becomes small, resulting in the reduction of absorption. In Fig. 4, we show the dependence of reflectivity and transverse shift on Ω_c . The reflectivity at resonance decreases initially with Ω_c and then increases gradually when the absorption exceeds a certain value. Accordingly, the reflection ratio $|r_s|/|r_p|$ as well as the magnitude of the transverse shift increases initially and then decreases. We can observe a significant enhancement of SHE when $|r_p|$ is extremely small. Due to the negative correlation between $\text{Im}(\varepsilon_3)$ and Ω_c [see Fig. 5(a)], Γ^{int} is larger than Γ^{rad} for small values of Ω_c and becomes less than Γ^{rad} when Ω_c is large [see Fig. 5(b)]. The transition Rabi frequency is about $\Omega_c \approx 2\Gamma$, around which there are large transverse shifts, and the direction of spin accumulation for the left-hand circular component changes from positive to negative as shown in Fig. 5(c). Because the transverse displacements of the two spin components are the same in magnitude and opposite in direction, the right-hand circular component can be controlled simultaneously.

In the above discussions, we have investigated the manipulation of photonic SHE in the case of a resonant driving

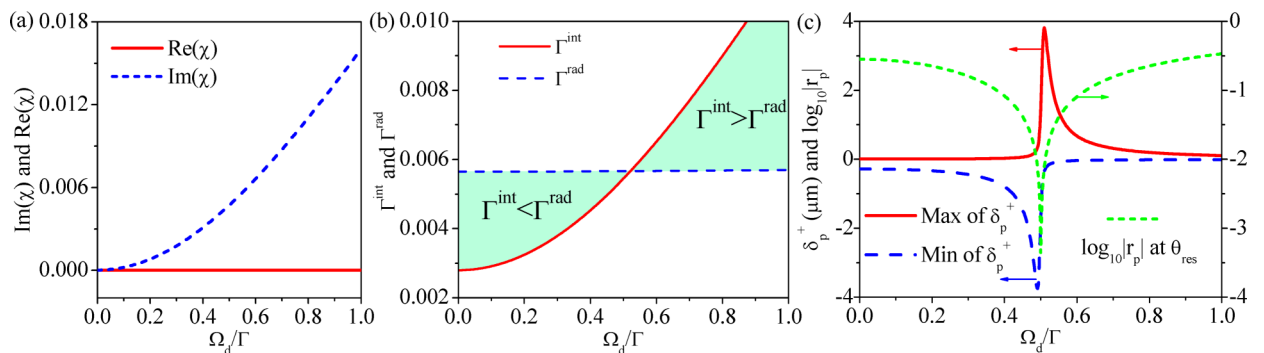


FIG. 3. (a) Probe susceptibility χ , (b) internal and radiation dampings Γ^{int} and Γ^{rad} , and (c) dip reflectivity and peak values of transverse shift δ_p^+ versus Rabi frequency of driving field Ω_d . Parameters are the same as those in Fig. 2.

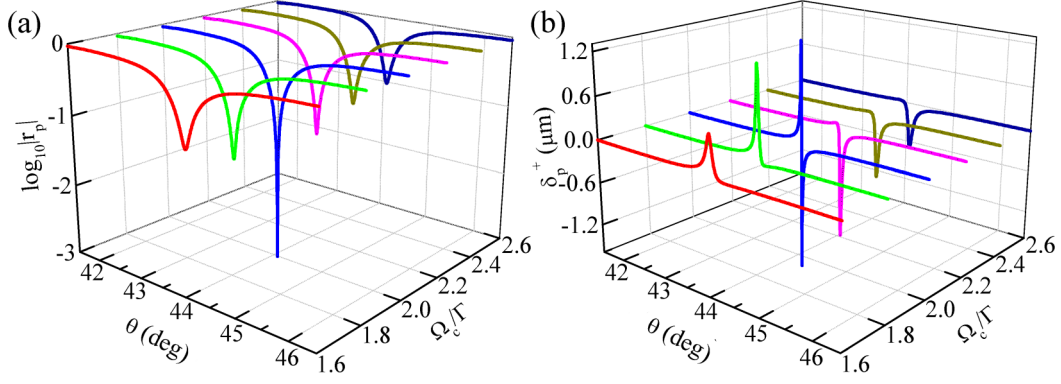


FIG. 4. (a) Reflectivity $|r_p|$ and (b) transverse shift of left-handed circularly polarized light δ_p^+ as a function of incident angle θ with various Rabi frequencies of coupling field Ω_c . The Rabi frequency of the driving field is $\Omega_d = 0.5\Gamma$, and other parameters are the same as those in Fig. 2.

field, and it can be seen that the resonance angle of SPR does not change. For some practical applications, such as beam steering, we hope that a large spin splitting can occur for light beams with different incident angles. Form Eq. (16), we can see that SPR occurs when $k_x = \text{Re}(k_x^0 + \Delta k_x)$. Generally, the condition $\text{Re}(k_x^0) \gg \text{Re}(\Delta k_x)$ is fulfilled. Then the resonance angle is mainly determined by $k_x = \text{Re}(k_x^0)$. Compared with the case when $\varepsilon_3 = 1$ (air or vacuum), the shift of resonance angle owing to the presence of a coherent medium is given by

$$\Delta\theta_{\text{res}} \approx \frac{\text{Re}(\chi)}{2\sqrt{\varepsilon_1} \cos\theta_0} \left(\frac{\varepsilon'_2}{\varepsilon'_2 + 1} \right)^{3/2}. \quad (22)$$

Here, θ_0 denotes the resonance angle of SPR when $\varepsilon_3 = 1$. Obviously, $\Delta\theta_{\text{res}}$ is proportional to the refractive part of the probe susceptibility and it provides a pathway to manipulate the peak position of the transverse displacement.

In order to obtain controllable $\text{Re}(\chi)$, the driving field should be off resonant with the transition $|2\rangle \leftrightarrow |4\rangle$. In the case of $\Delta_d = 40\Gamma$, we show the reflection and the transverse shift spectra for various values of Ω_d in Figs. 6(a) and 6(b). The reflection dip becomes narrow and sharp with increasing Ω_d . However, on exceeding a certain value, it becomes wide and shallow. The transverse shift displays similar changes. On comparing with Fig. (2), we find that there is a change in the resonant angle owing to the variation of the refractive index of the coherent medium. In the absence of the driving field, the medium is transparent to the probe field as a result of

destructive quantum interference [4–6]. When a driving field with large detuning is applied, it introduces a small perturbation to the state $|2\rangle$ as a consequence of the ac-Stark effect. This makes the Λ -type system deviate slightly from the two-photon resonance. Then both absorptive and refractive parts of the probe susceptibility can be simultaneously controlled by the driving field. In the case of $\Delta_p = \Delta_c = 0$ and $\gamma_{21} \approx 0$, the probe susceptibility can be written as

$$\chi = -\frac{\mathcal{N}\Omega_d^2}{\Omega_c^2\Delta_d} + i\frac{\mathcal{N}\Omega_d^2}{2\Omega_c^2\Delta_d^2} \left(\Gamma_4 + \frac{\Omega_d^2\Gamma_3}{\Omega_c^2} \right). \quad (23)$$

Obviously, $\text{Re}(\chi)$ is proportional to Ω_d^2 , and hence corresponds to the third-order Kerr nonlinearity [see Fig. 6(c)]. As a result, the resonance angle of SPR varies almost linearly with the driving field intensity as shown in Fig. 6(d1). Meanwhile, the absorption of the medium as well as the internal damping of the system increases nonlinearly with Ω_d^2 . Around the optimal value of Ω_d where $\Gamma^{\text{int}} = \Gamma^{\text{rad}}$, large positive and negative spin splittings can be observed. Then, we can manipulate the magnitude, sign, and peak position of transverse displacement by a detuned driving field.

When the driving field is off resonant, the coupling field has influence on the probe susceptibility as well. According to Eq. (23), $\text{Re}(\chi)$ is inversely proportional to Ω_c^2 , and then the resonance angle of SPR depends linearly on Ω_c^{-2} . Figures 7(a1), 7(a2), 7(b1), and 7(b2) verify these results. For a positive detuning ($\Delta_d > 0$), the slope of the $\text{Re}(\chi) - \Omega_c^{-2}$

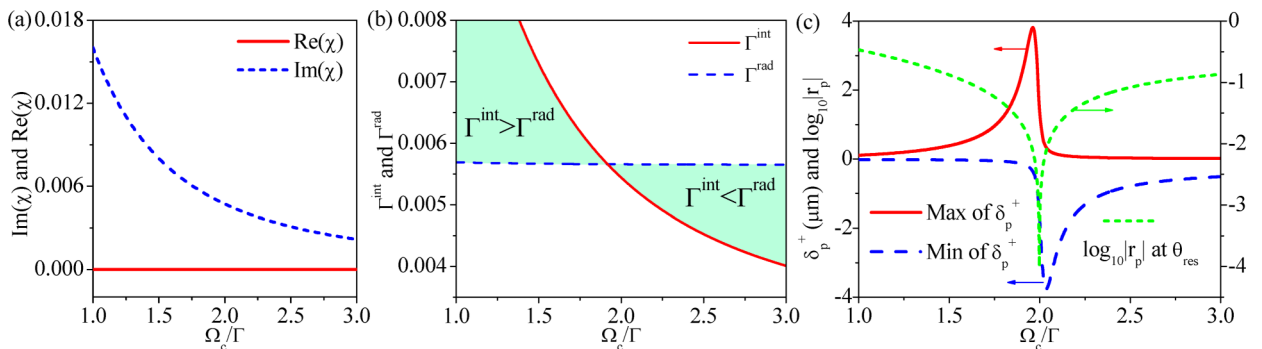


FIG. 5. (a) Probe susceptibility χ , (b) internal and radiation dampings Γ^{int} and Γ^{rad} , and (c) dip reflectivity and peak values of transverse shift δ_p^+ versus Rabi frequency of driving field Ω_d . Parameters are the same as those in Fig. 4.

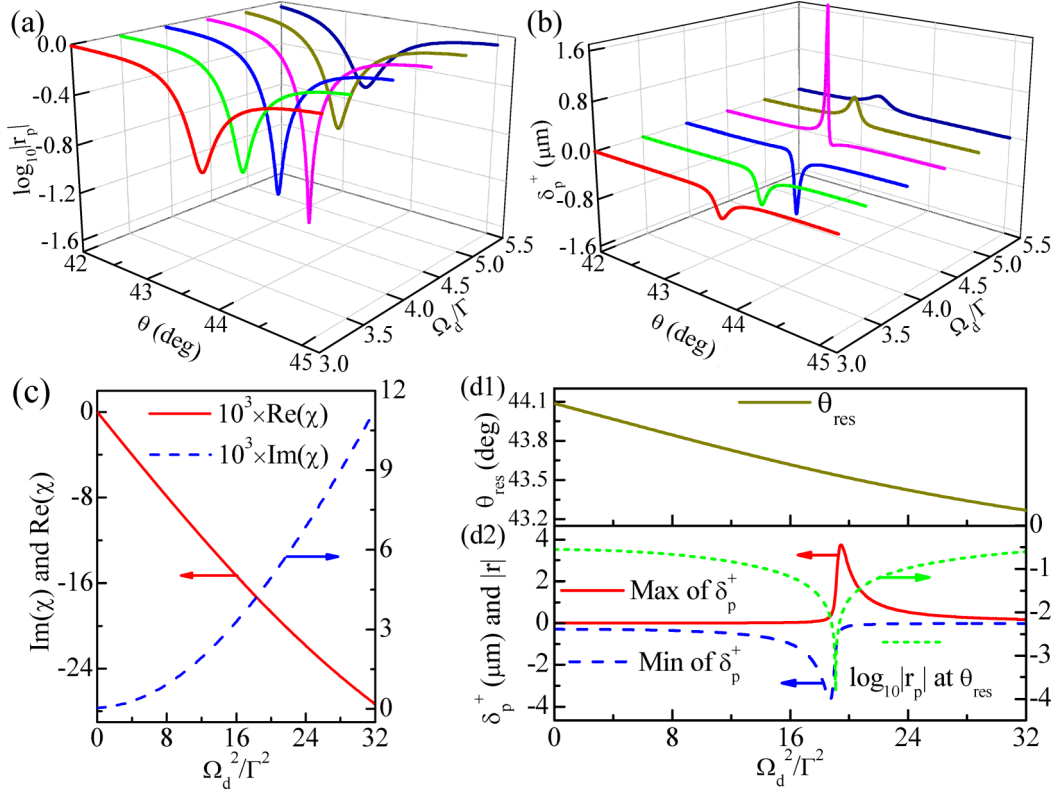


FIG. 6. (a) Reflectivity $|r_p|$ and (b) transverse shift δ_p^+ as a function of incident angle θ with various Rabi frequencies of driving field Ω_d . (c) Probe susceptibility χ , (d1) resonance angle θ_{res} , and (d2) dip reflectivity and peak values of δ_p^+ versus Ω_d^2 . Parameters are $\Omega_c = \Gamma$, $\Delta_d = 40\Gamma$, and other parameters are the same as those in Fig. 3.

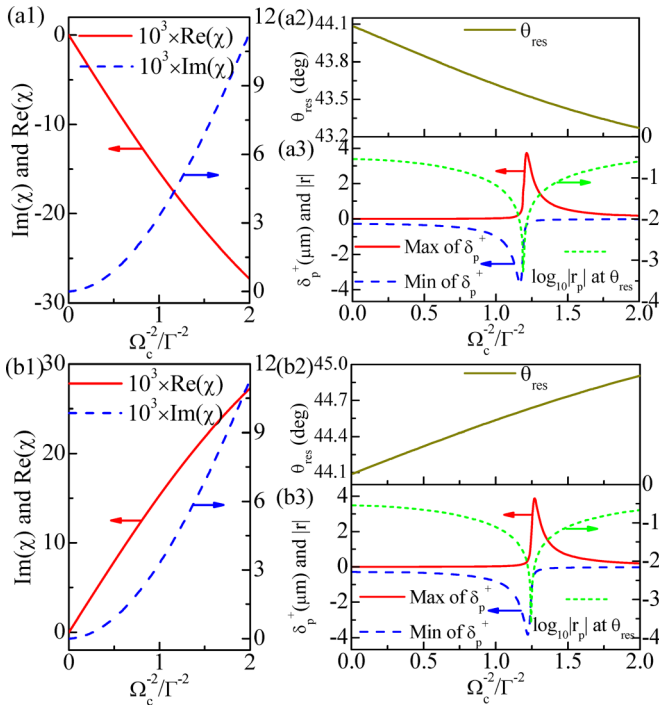


FIG. 7. Probe susceptibility χ , resonance angle θ_{res} , reflectivity at θ_{res} , and maximum (minimum) of δ_p^+ versus Ω_c^{-2} . Parameters are $\Omega_d = 4\Gamma$, $\Delta_d = 40\Gamma$ for (a1–a3), and $\Delta_d = -40\Gamma$ for (b1–b3). Other parameters are the same as those in Fig. 3.

curve is negative, and then the resonance angle decreases linearly with the increase of Ω_c^{-2} [see Fig. 7(a2)]. On the contrary, θ_{res} increases with Ω_c^{-2} when $\Delta_d < 0$ [see Fig. 7(b2)]. In addition, the absorption of the medium is dependent on Δ_d^2 , and then the variation tendencies of dip reflectivity and transverse shift versus Ω_c are similar for the cases of $\Delta_d = 40\Gamma$ and $\Delta_d = -40\Gamma$. However, there is a small difference in the values of Ω_c for zero reflection (i.e., $\Gamma^{\text{int}} = \Gamma^{\text{rad}}$), because the contribution of $\text{Re}(\chi)$ is neglected in the derivation of Eq. (20).

IV. CONCLUSION

In conclusion, we have investigated the SHE of light upon reflection from a three-layer Kretschmann configuration in which the metal film is backed by a coherent atomic medium. The photonic SHE can be enhanced as a result of a large ratio of reflection coefficients for the TE and TM modes in the presence of SPR. The minimum reflectivity of TM-polarized light is related to the internal damping of the structure and depends directly on the absorption of the medium. By adjusting the parameters of the laser fields in an N -type atomic system, the reflection ratio can be coherently controlled and greatly improved when the internal damping approaches the radiation damping. Then we can observe significantly enhanced photonic SHE. Meanwhile, the direction of spin accumulations can be switched by modulating the adsorption. As the internal damping becomes larger than the radiation damping, the

left-hand circular component undergoes positive transverse shift. In the opposite case, we obtain a negative shift. The peak of the transverse shift appears around the resonance angle of SPR, which depends on the refractive part of the susceptibility of the medium and can be coherently controlled in the case of an off-resonant driving field. Therefore, with the assistance of a coherent medium, we can conveniently manipulate the magnitude and direction as well as the peak position of transverse displacement. The control of photonic SHE is based on the tunable complex susceptibility via the atomic coherence effect. It is much more efficient than other SPR schemes where the tuning of transverse shift is achieved by changing the structure. The flexible control of the spin-dependent

splitting may have potential applications in nanophotonic devices.

ACKNOWLEDGMENTS

This work is supported by Natural National Science Foundation of China (NSFC) (Grant No. 11204367), Natural Science Basic Research Plan in Shaanxi Province (Grant No. 2018JQ1051), Fundamental Research Funds for the Central Universities (Grant No. GK202003021), and Scholarship Program of China Scholarship Council (Grant No. 201806875036). This research is also supported by a grant from King Abdulaziz City of Science and Technology (KACST).

-
- [1] M. O. Scully, S. Y. Zhu, and A. Gavrielides, *Phys. Rev. Lett.* **62**, 2813 (1989).
- [2] J. Y. Gao, C. Guo, X. Z. Guo, G. X. Jin, Q. W. Wang, J. Zhao, H. Z. Zhang, Y. Jiang, D. Z. Wang, and D. M. Jiang, *Opt. Commun.* **93**, 323 (1992).
- [3] Y. F. Zhu, *Phys. Rev. A* **45**, R6149 (1992).
- [4] K. J. Boller, A. Imamoglu, and S. E. Harris, *Phys. Rev. Lett.* **66**, 2593 (1991).
- [5] M. Fleischhauer, A. Imamoglu, and J. P. Marangos, *Rev. Mod. Phys.* **77**, 633 (2005).
- [6] M. O. Scully and M. S. Zubairy, *Quantum Optics* (Cambridge University, Cambridge, 1997).
- [7] O. Schmidt, R. Wynands, Z. Hussein, and D. Meschede, *Phys. Rev. A* **53**, R27 (1996).
- [8] L. V. Hau, S. E. Harris, Z. Dutton, and C. H. Behroozi, *Nature* **397**, 594 (1999).
- [9] M. M. Kash, V. A. Sautenkov, A. S. Zibrov, L. Hollberg, G. R. Welch, M. D. Lukin, Y. Rostovtsev, E. S. Fry, and M. O. Scully, *Phys. Rev. Lett.* **82**, 5229 (1999).
- [10] M. Fleischhauer and M. D. Lukin, *Phys. Rev. Lett.* **84**, 5094 (2000).
- [11] Y. Wu and L. Deng, *Phys. Rev. Lett.* **93**, 143904 (2004).
- [12] G. X. Huang, L. Deng, and M. G. Payne, *Phys. Rev. E* **72**, 016617 (2005).
- [13] C. Ottaviani, D. Vitali, M. Artoni, F. Cataliotti, and P. Tombesi, *Phys. Rev. Lett.* **90**, 197902 (2003).
- [14] Y. P. Niu, S. Q. Gong, R. X. Li, Z. Z. Xu, and X. Y. Liang, *Opt. Lett.* **30**, 3371 (2005).
- [15] Z. B. Wang, K. P. Marzlin, and B. C. Sanders, *Phys. Rev. Lett.* **97**, 063901 (2006).
- [16] D. A. Braje, V. Balić, S. Goda, G. Y. Yin, and S. E. Harris, *Phys. Rev. Lett.* **93**, 183601 (2004).
- [17] Y. P. Zhang, A. W. Brown, and M. Xiao, *Phys. Rev. Lett.* **99**, 123603 (2007).
- [18] Y. F. Mei, X. X. Guo, L. W. Zhao, and S. W. Du, *Phys. Rev. Lett.* **119**, 150406 (2017).
- [19] L. G. Wang, M. Ikram, and M. S. Zubairy, *Phys. Rev. A* **77**, 023811 (2008).
- [20] Ziauddin, S. Qamar, and M. S. Zubairy, *Phys. Rev. A* **81**, 023821 (2010).
- [21] H. R. Hamed, A. Radmehr, and M. Sahrai, *Phys. Rev. A* **90**, 053836 (2014).
- [22] Ziauddin, Y. L. Chuang, and R. K. Lee, *Phys. Rev. A* **92**, 013815 (2015).
- [23] X.-J. Zhang, H.-H. Wang, Z.-P. Liang, Y. Xu, C.-B. Fan, C.-Z. Liu, and J.-Y. Ga, *Phys. Rev. A* **91**, 033831 (2015).
- [24] T. Shui, W. X. Yang, Q. Y. Zhang, X. Liu, and L. Li, *Phys. Rev. A* **99**, 013806 (2019).
- [25] F. Goos and H. Hänchen, *Ann. Phys.* **436**, 333 (1947).
- [26] M. Onoda, S. Murakami, and N. Nagaosa, *Phys. Rev. Lett.* **93**, 083901 (2004).
- [27] K. Yu. Bliokh and Y. P. Bliokh, *Phys. Rev. Lett.* **96**, 073903 (2006).
- [28] K. Yu. Bliokh and Y. P. Bliokh, *Phys. Rev. E* **75**, 066609 (2007).
- [29] F. I. Fedorov, *Dokl. Akad. Nauk SSSR* **105**, 465 (1955).
- [30] C. Imbert, *Phys. Rev. D* **5**, 787 (1972).
- [31] O. Hosten and P. Kwiat, *Science* **319**, 787 (2008).
- [32] Y. Qin, Y. Li., H. Y. He, and Q. H. Gong, *Opt. Lett.* **34**, 2551 (2009).
- [33] H. L. Luo, X. X. Zhou, W. X. Shu, S. C. Wen, and D. Y. Fan, *Phys. Rev. A* **84**, 043806 (2011).
- [34] H. L. Luo, S. C. Wen, W. X. Shu, and D. Y. Fan, *Phys. Rev. A* **82**, 043825 (2010).
- [35] H. L. Luo, X. H. Ling, X. X. Zhou, W. X. Shu, S. C. Wen, and D. Y. Fan, *Phys. Rev. A* **84**, 033801 (2011).
- [36] B. Wang, Y. Li, M.-M. Pan, J.-L. Ren, Y.-F. Xiao, H. Yang, and Q. Gong, *Phys. Rev. A* **88**, 043842 (2013).
- [37] T. T. Tang, J. Li, Y. F. Zhang, C. Y. Li, and L. Luo, *Opt. Express* **24**, 28113 (2016).
- [38] X. Jiang, Q. K. Wang, J. Guo, J. Zhang, S. Q. Chen, X. Y. Dai, and Y. J. Xiang, *J. Phys. D* **51**, 145104 (2018).
- [39] X. X. Zhou, Z. C. Xiao, H. L. Luo, and S. C. Wen, *Phys. Rev. A* **85**, 043809 (2012).
- [40] W. G. Zhu and W. L. She, *Opt. Lett.* **40**, 2961 (2015).
- [41] M. J. Jiang, W. G. Zhu, H. Y. Guan, J. H. Yu, H. H. Lu, J. Y. Tan, J. Zhang, and Z. Chen, *Opt. Lett.* **42**, 3259 (2017).
- [42] X. B. Yin, Z. L. Ye, J. Rho, Y. Wang, and X. Zhang, *Science* **339**, 1405 (2013).
- [43] A. Shaltout, J. J. Liu, A. Kildishev, and V. Shalaev, *Optica* **2**, 860 (2015).
- [44] W. J. M. Kort-Kamp, N. A. Sinitsyn, and D. A. R. Dalvit, *Phys. Rev. B* **93**, 081410(R) (2016).
- [45] L. Cai, M. X. Liu, S. Z. Chen, Y. C. Liu, W. X. Shu, H. L. Luo, and S. C. Wen, *Phys. Rev. A* **95**, 013809 (2017).

- [46] X. X. Bai, L. L. Tang, W. Q. Lu, X. Z. Wei, S. Liu, Y. Liu, X. D. Sun, H. F. Shi, and Y. G. Lu, *Opt. Lett.* **42**, 4087 (2017).
- [47] L. Salasnich, *Phys. Rev. A* **86**, 055801 (2012).
- [48] X. X. Zhou and X. H. Ling, *IEEE Photonics J.* **8**, 1 (2016).
- [49] X. J. Tan and X. S. Zhu, *Opt. Lett.* **41**, 2478 (2016).
- [50] Y. J. Xiang, X. Jiang, Q. You, J. Guo, and X. Y. Dai, *Photonics Res.* **5**, 467 (2017).
- [51] S. Asiri, J. P. Xu, M. Al-Amri, and M. S. Zubairy, *Phys. Rev. A* **93**, 013821 (2016).
- [52] X. J. Zhang, H. H. Wang, C. Z. Liu, G. W. Zhang, L. Wang, and J. H. Wu, *Opt. Express* **25**, 10335 (2017).